Open Research Online

The Open University's repository of research publications
and other research outputs

Backcalculation of keratometer index based on OCT data and raytracing – a Monte Carlo simulation

Journal Item

How to cite:

Langenbucher, Achim; Szentmáry, Nóra; Weisensee, Johannes; Cayless, Alan; Menapace, Rupert and Hoffmann, Peter (2021). Backcalculation of keratometer index based on OCT data and raytracing – a Monte Carlo simulation. Acta Ophthalmologica, 99(8) pp. 843–849.

For guidance on citations see FAQs.

© 2021 Achim Langenbucher; 2021 Nóra Szentmáry; 2021 Johannes Weisensee; 2021 Alan Cayless; 2021 Rupert Menapace; 2021 Peter Hoffmann

https://creativecommons.org/licenses/by/4.0/

Version: Version of Record

Link(s) to article on publisher's website:
http://dx.doi.org/doi:10.1111/aos.14794

Copyright and Moral Rights for the articles on this site are retained by the individual authors and/or other copyright owners. For more information on Open Research Online's data policy on reuse of materials please consult the policies page.

oro.open.ac.uk

Acta Ophthalmologica

Back-calculation of keratometer index based on OCT data and raytracing – a Monte Carlo simulation

Achim Langenbucher,[1] Nóra Szentmáry,[2,3] Johannes Weisensee,[1] Alan Cayless,[4] Rupert Menapace[5] and Peter Hoffmann[6]

[1]Department of Experimental Ophthalmology, Saarland University, Homburg/Saar, Germany
[2]Dr. Rolf M. Schwiete Center for Limbal Stem Cell and Aniridia Research, Saarland University, Homburg/Saar, Germany
[3]Department of Ophthalmology, Semmelweis-University, Budapest, Hungary
[4]School of Physical Sciences, The Open University, Milton Keynes, UK
[5]Department of Ophthalmology, Vienna University, Vienna, Austria
[6]Augen- und Laserklinik Castrop-Rauxel, Castrop-Rauxel, Germany

ABSTRACT.

Purpose: **This study aims to develop a raytracing-based strategy for calculating corneal power from anterior segment optical coherence tomography data and extracting the individual keratometer index, which converts the corneal front surface radius to corneal power.**

Methods: **A large OCT dataset (10,218 eyes of 8,430 patients) from the Casia 2 (Tomey, Japan) was post-processed in MATLAB (MathWorks, USA). Radius of curvature, asphericity of the corneal front and back surface, central corneal thickness and pupil size (aperture) were used to trace a bundle of rays through the cornea and derive the best focus plane. Corneal power was calculated with respect to the corneal front vertex plane, and the keratometer index was back-calculated using corneal power and front surface radius. Keratometer index was analysed in a multivariate linear model.**

Results: **The averaged resulting keratometer index was 1.3317 ± 0.0017 with a median of 1.3317 and range from 1.3233 to 1.3390. In a univariate model, only the front surface asphericity affected the keratometer index. The multivariate model for modelling the keratometer index using all 6 input parameters performed very well (RMS error: 5.54e-4, R^2: 0.90, significance vs. constant model: <0.0001).**

Conclusions: **In the classical calculation, the keratometer index used for converting corneal radius to dioptric power uses several model assumptions. As these assumptions are not generally satisfied, corneal power cannot be calculated from corneal front surface radius alone. Considering all 6 input variables, the linear prediction model performs well and can be used if all input parameters are measured with a tomographer.**

Key words: calculation scheme – corneal power – Monte Carlo simulation – optical coherence tomography – raytracing

Acta Ophthalmol.

© 2021 The Authors. Acta Ophthalmologica published by John Wiley & Sons Ltd on behalf of Acta Ophthalmologica Scandinavica Foundation.
This is an open access article under the terms of the Creative Commons Attribution License, which permits use, distribution and reproduction in any medium, provided the original work is properly cited.

doi: 10.1111/aos.14794

Background

Corneal power is one of the most important parameters for calculating the power of lens implants (Olsen 1986; Preussner, Wahl & Weitzel 2005), but it cannot be measured in situ. The power of a lens is always defined by the reciprocal of the focal length corrected for the refractive index of the optical media, and the focal length has to be referenced either to the image side principal plane (so-called equivalent power of the lens) or to the front or back vertex (so-called front vertex or back vertex power). Instead of measuring corneal power directly, clinicians measure the shape of the corneal surfaces and estimate corneal power based on a simplified optical model (Olsen & Jeppesen 2018). Most cases are restricted to a measurement of radius of curvature of the corneal front surface (R_a) using, for example a keratometer or a corneal topographer (Olsen & Jeppesen 2018; Langenbucher et al. 2020). Based on any schematic model eye, corneal front surface radius can be converted into corneal power using assumptions such as a fixed ratio of corneal front surface radius to back surface radius (R_b) and a fixed corneal thickness (CCT), and refractive indexes of cornea and aqueous humour. It is obvious that in situations where the proportions do not properly match the underlying model such a conversion results in incorrect values for corneal

power, which – inserted in a lens power calculation scheme – yields inappropriate results for the power of the lens and a refractive surprise after cataract surgery (Olsen 1986; Langenbucher, Haigis & Seitz 2004; Preussner, Wahl & Weitzel 2005; Haigis 2012).

With modern tomography techniques, the shape of the cornea can be assessed with a high precision (Ho et al. 2008; Olsen & Jeppesen 2018). In particular, Scheimpflug tomographers with or without integrated Placido topography and high-resolution optical coherence tomographers (OCT) permit measurements of corneal front and back surface curvature as well as asphericity and corneal thickness with a high degree of accuracy and reliability. The refractive indices of the cornea and aqueous humour cannot be directly measured *in situ*, but for both parameters the variation seems to be quite low, and most schematic model eyes describe congruent data with n_C = 1.376 for the cornea and n_{AQ} = 1.336 for the aqueous humour (Liou & Brennan 1997).

In clinical routine, conversion of corneal front surface radius R_a to corneal power CP is performed with a keratometer index n_K, which is an assumed parameter or calibration value (Olsen 1986; Fam & Kim 2007; Langenbucher et al. 2020). In many keratometers or topographers, the conversion is hard-coded meaning that the user cannot modify the keratometer index (Langenbucher, Haigis & Seitz 2004; Haigis 2012). The formula behind reads.

$$n_K = 1 + CP \cdot R_a.$$

Several different values are used, including the so-called Javal index with n_K = 1.3375 and the Zeiss index with n_K = 1.332 which are the most popular calibrations (Olsen 1986; Fam & Lim 2007; Olsen & Jeppesen 2018). Interpreting these two keratometer indices based on the Gullstrand schematic model eye, the Javal index refers to the back vertex power and the Zeiss index to the front vertex power of the cornea. This results in a difference between R_a converted to CP using the Javal, and the Zeiss index is around 0.75 dioptres on average (Langenbucher et al. 2020). This means that these two calibrations cannot be used interchangeably, and if a lens power calculation scheme is designed to use CP instead of R_a the user should check carefully which calibration should be used.

Even if the radius of curvature of both corneal surfaces together with central corneal thickness is measured, and a thick lens formula used for calculation of corneal power, the calculation is mostly performed with restrictions of linear Gaussian optics (in the paraxial space), and the asphericity of the front (Q_a) and back surface (Q_b) and the aperture of the eye (PUP) are not taken into account.

The purpose of this study was to assess corneal power and back-calculated keratometer index based on a large dataset of high-resolution anterior segment OCT using raytracing techniques in terms of a Monte Carlo simulation, and to present the results for back-calculated keratometer index as a function of corneal front and back surface radius, asphericity of corneal front and back surface, corneal thickness and pupil size.

Methods

Measurement data

Out of a total of 11,276 measurements in patients without pathologies or a history of ocular surgery performed between January 2019 and July 2020, 10,218 OCT measurements with a complete set of data (10,218 eyes of 8,430 patients) were enrolled in this study. In all of these measurements, the internal quality check of the tomographer indicated a proper measurement and no movement artefacts. All measurements were carried out at Augenklinik Castrop-Rauxel. An ethics approval was not required for this study. This study is a retrospective evaluation of data which were collected during routine examinations. No extra examinations or measurements were performed.

The data were transferred to us in an anonymized fashion, which precludes back-tracing of the patient.

Data from the Casia 2 (Tomey, Nagoya, Japan) were exported in standard.csv data format and imported to MATLAB (MathWorks, Natick, USA, Version 2019b) for subsequent data analysis. From the dataset, we used the central corneal front surface radius R_a, the central corneal back surface radius R_b, corneal eccentricity of the corneal front (ECC_a) and back surface (ECC_b) both derived in the central 6 mm zone, central corneal thickness CCT and projected (visible) pupil size. Corneal eccentricity with a positive value in the dataset indicating a prolate shape of the corneal surface was converted to corneal asphericity using.

$$Q_{a,b} = -(\mathrm{ECC}_{a,b})^2.$$

Corneal surfaces with an oblate shape indicated in the dataset with a negative value of eccentricity were converted to

$$Q_{a,b} = (\mathrm{ECC}_{a,b})^2.$$

Calculation scheme

We assumed a centred optical system without any tilt of the 2 corneal surfaces. Both surfaces were considered as quadric surfaces described by a central radius of curvature (R_a or R_b) and an asphericity (Q_a and Q_b). The axial symmetry of this model means that restriction to a 2-dimensional raytracing strategy was sufficient (Langenbucher et al. 2006; Langenbucher et al. 2011; Langenbucher et al. 2014; Langenbucher et al. 2016). The apex of the corneal front surface was assumed to be located at $z = 0$ and the corneal back surface apex at a distance of z = CCT.

A collimated bundle of 601 rays starting from a plano surface at $z = 0$ (apex plane of the cornea) was projected to each cornea where the radial ray spacing was adapted in a quadratic fashion from centre to periphery to realize an equally spaced sampling over the pupil size (area-correction). The diameter of the ray bundle was adjusted to the measured diameter of the pupil PUP. Then, the ray-surface intersection was calculated and the direction of the refracted rays was derived using Snell's law for the corneal front surface (Langenbucher et al. 2006; Langenbucher et al. 2011; Langenbucher et al. 2014; Langenbucher et al. 2016). After tracing all rays through the cornea, ray intersection with the corneal back surface was calculated and the direction of the refracted rays in the anterior chamber was derived using the Snell's law. The best focus plane $z = z_F$ was determined based on the criterion of least scatter

(root mean squared error). A non-linear search algorithm (Levenberg–-Marquardt algorithm (Levenberg 1944; Marquardt 1963); maximum iterations: 100; termination tolerance on the function value: 1e-16; termination tolerance for the step size; 1e-14) was used for calculating the best focus (Langenbucher et al. 2006).

At best focus plane $z = z_F$, the cumulative optical path length was calculated for each ray starting from object plane $z = 0$, and the standard deviation of optical path length for all rays in the ray bundle was used as a measure for optical aberration (Langenbucher et al. 2006). From the best focus plane z_F, we assessed corneal power referenced to the corneal front vertex plane (as this surface is the reference for biometry prior to cataract surgery) and back-calculated the individual keratometer index from z_F and R_a.

Data from the $N = 10{,}218$ eyes were analysed descriptively using mean, standard deviation (SD), median, minimum and maximum. We then investigated the data pool using different multiple linear regression models (Model 1: Multivariate linear model using all 6 input parameters R_a, R_b, Q_a, Q_b, CCT and PUP; Model 2: Simplified linear model with three parameters R_a, R_b and CCT; Model 3: Simple linear model based on a single parameter (corneal front surface radius model R_a) to investigate the overall performance of the models as well as the regression coefficients, standard errors and the relevance (P-value) of the effect sizes. Finally, we plotted the back-calculated keratometer index as a function of R_a, R_b, Q_a, Q_b, CCT and PUP.

Results

The descriptive statistics of the 6 input data of R_a, R_b, Q_a, Q_b, CCT and PUP is shown in Table 1.

In Fig. 1, we have plotted the histogram of the distribution for all $N = 10{,}218$ input data.

Table 2 displays the descriptive statistics for the output variables: position of the best focus z_F, corneal power CP, root mean squared error of optical path length differences and back-calculated keratometer index.

Figure 2 provides a histogram of the distribution of the best focus plane z_F, the corneal power CP referenced to the front vertex plane of the cornea and the back-calculated keratometer index n_K.

The results of the linear model for estimation of the keratometer index from all 6 input parameters R_a, R_b, Q_a, Q_b, CCT and PUP yield:

$$n_K = 1.33 - 3.79e\text{-}3 \cdot R_a + 6.60e\text{-}3 \cdot Q_a + 3.96e\text{-}3 \cdot R_b - 1.20e\text{-}3 \cdot Q_b + 1.60e\text{-}6 \cdot CCT + 4.49e\text{-}4 \cdot PUP \text{ (model 1)}$$

The root mean squared error/R^2/significance vs. a constant model is 5.54e-4/8.98e-1/<0.0001. The standard errors of the regression coefficients are 1.76e-4 for the intercept and 3.32e-5/2.37e-5/3.43e-5/2.73e-5/1.52e-7/7.23e-6 for R_a/Q_a/R_b/Q_b/CCT/PUP. The significance level of all 6 effect sizes and the intercept is lower than 6.44e-15.

The simplified linear model for estimation of the keratometer index from the input data used for a paraxial back-calculation of the corneal power as a thick lens R_a, R_b, and CCT yields:

$$n_K = 1.33 - 1.90e\text{-}3 \cdot R_a + 2.41e\text{-}3 \cdot R_b - 2.11e\text{-}7 \cdot CCT \text{ (model 2)}$$

The root mean squared error/R^2/significance vs. a constant model is 1.69e-3/5.50e-2/<0.0001. This model is not appropriate for estimation of the keratometer index. The standard error of the regression coefficients are 5.30e-4 for the intercept and 9.91e-5/1.02e-4/4.61e-4 for R_a/R_b/CCT. The significance level of the 3 effect sizes and the intercept is lower than 1e-16.

If calculating the keratometer index with a linear model based only on the corneal front surface radius model R_a, the model description reads as follows:

$$n_K = 1.33 - 3.77e\text{-}4 \cdot R_a \text{ (model 3)}$$

The root mean squared error/R^2/significance vs. a constant model is 1.66e-3/4.00e-3/0.229. This model is not appropriate for estimation of the keratometer index. The standard errors of the regression coefficients are 6.15e-4 for the intercept and 7.96e-5 for R_a. The significance level of the R_a as effect sizes and the intercept is lower than 1e-16.

Figure 3 shows the back-calculated keratometer index as a function of corneal front surface radius R_a (Fig. 3 A), corneal front surface asphericity Q_a (Fig. 3B), corneal back surface radius R_b (Fig. 3C), corneal back surface asphericity Q_b (Fig. 3D), central corneal thickness CCT (Fig. 3E) and pupil size PUP (Fig. 3F). If we restrict to a linear estimation model with one effect size, only the asphericity of the corneal front surface Q_a (Fig. 3B) appears to be a good predictor for the keratometer index. In all graphs, we have included the linear fit in terms of minimizing the squared fit error. The respective slope of the fit is provided in the legend of each graph. Due to the special characteristics of the data distribution in Fig. 3B, we added a sigmoidal function which is defined by the lower/upper boundary of 1.3260/1.3345, an inflection point at $Q_a = -0.4895$ and a slope at the inflection point of 3.9537. The linear and the sigmoidal model both yielded a comparable fitting performance with a root mean squared fit error of 1.38e-3 and 1.36e-3, respectively.

Discussion

There is always discussion in the community of cataract surgeons about the proper keratometer index (Olsen 1986; Preussner, Wahl & Weitzel 2005; Fam & Lim 2007; Olsen & Jeppesen 2018). If we keep in mind that the basic measure is the shape of the corneal front surface, corneal power is always a result of a conversion from corneal front surface radius alone (e.g. keratometer), of corneal front and back surface radius together with central corneal thickness [e.g. thick lens formula with linear Gaussian optics

Table 1. Descriptive statistics of the input data with mean, standard deviation (SD), median, minimum and maximum. R_a refers to the corneal front surface radius, Q_a to the corneal front surface asphericity, R_b to the corneal back surface radius, Q_b to the corneal back surface asphericity, CCT to the central corneal thickness and PUP to the pupil size considered at the corneal plane

$N = 10.218$	R_a in mm	Q_a	R_b in mm	Q_b	CCT in µm	PUP in mm
Mean	7.733	−0.3141	6.534	−0.007	547	4.408
SD	0.283	0.249	0.274	0.213	37	0.789
Median	7.720	−0.319	-6.530	−0.014	547	4.468
Minimum	6.770	−1.486	5.500	−0.988	395	1.528
Maximum	8.800	0.584	7.500	0.602	794	6.800

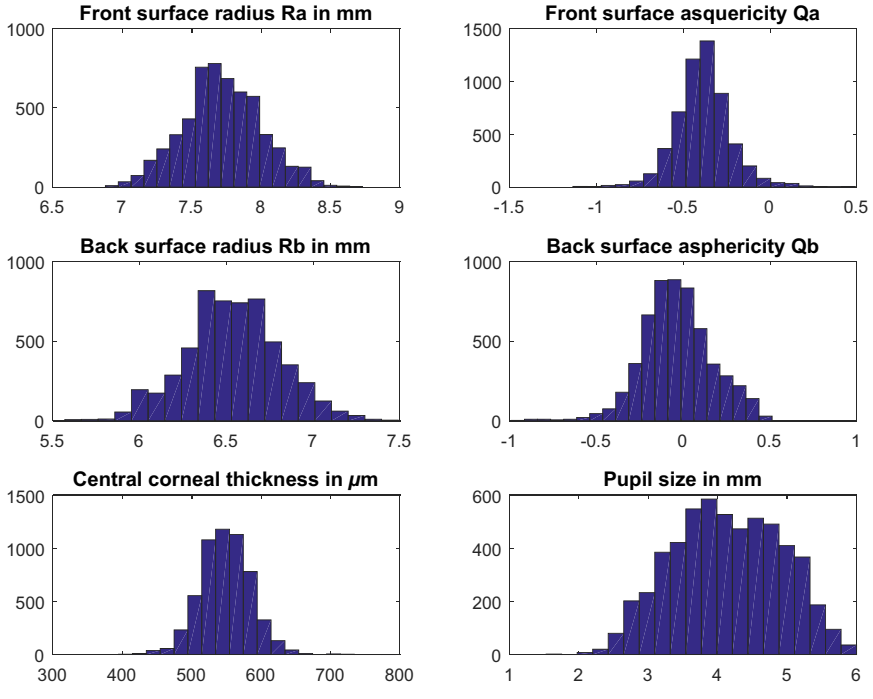

Fig. 1. Histogram of the distribution of input parameters (N = 10,218). R_a refers to the corneal front surface radius, Q_a to the corneal front surface asphericity, R_b to the corneal back surface radius, Q_b to the corneal back surface asphericity, CCT to the central corneal thickness and PUP to the pupil size.

Table 2. Descriptive statistics of the output data with mean, standard deviation (SD), median, minimum and maximum. z_F refers to the position of the best focus in terms of lowest ray scatter, CP to the corneal power with respect to the corneal front vertex plane, SD OPL to the standard deviation of optical path length differences from the object plane $z = 0$ to the best focus plane $z = z_F$ and n_K to the back-calculated keratometer index

N = 10.218	z_F in mm	CP in dioptres	SD OPL in μm	n_K
Mean	31.177	42.914	0.185	1.3317
SD	1.192	1.637	0.168	0.0017
Median	31.126	42.922	0.131	1.3317
Minimum	27.113	37.104	0.000	1.3233
Maximum	36.007	49.275	0.938	1.339

(Langenbucher et al. 2020)] or of raytracing strategies [e.g. using radius of curvature for the front and back surface, asphericity of the front and back surface, central cornel thickness, and diameter of the aperture or a full set of tomographic data (Preussner, Wahl & Weitzel 2005)]. Measurement of corneal power is not possible if the cornea is *in situ*. If interpreting a corneal shape during conversion to corneal power, we require a supporting optical model which provides the refractive indices of corneal tissue and aqueous humour (Liou & Brennan 1997), and if we do not use a full set of tomographic data we must make some assumptions which are typically derived from the schematic model eye. As an example, the Zeiss and the Javal index are both based on the classical Gullstrand model eye, and the derivation of both keratometer indices involves the use of the ratio between corneal front to back surface curvature and corneal thickness (Langenbucher, Haigis & Seitz 2004; Haigis 2012). The difference between the Zeiss and Javal index is primarily that the two indices refer to a different reference plane.

With modern optical measurement techniques, we get accurate and reproducible measures of the entire corneal shape including front surface and back surface architecture and central thickness. Therefore, it is obvious to use these measurement data to upgrade determination of corneal power and to question the traditional keratometer index. We extracted a large dataset of anterior segment OCT data from normal eyes measured in the last 18 months at one clinical centre in Germany. Based on this dataset and an estimate of the refractive index for the cornea and aqueous humour, we used raytracing techniques to calculate the best focus plane. As we used a concentric optical model based on the assumptions that both corneal surfaces are aligned and perpendicular to the fixation axis, we could restrict the analysis to a 2D raytracing strategy instead of 3D raytracing which is more complex and time-consuming. If we were to trace an equidistant bundle of rays (in one meridian) through the cornea, the data would be much denser in the centre and sparser in the periphery. Therefore, we decided to adapt the ray density in a quadratic fashion to resample a homogeneous distribution over the entire pupil. The further data processing was performed in a similar way to a classical Monte Carlo simulation. The back-calculated keratometer index for all eyes was analysed as a function of all potential effect sizes (R_a, R_b, Q_a, Q_b, CCT and PUP) separately, and after that multivariate linear models were defined which simplify the raytracing calculation and make a linear prediction for the appropriate keratometer index to be used for translating corneal front surface curvature to a corneal power. In total, 3 multivariate linear models were described, one of them considering all 6 potential effect sizes, one considering 3 effect sizes (R_a, R_b and CCT) and one as a simple linear model with one effect size (R_a) only).

For the model that we present in this paper, we used a collimated bundle of rays starting from the corneal front vertex plane and traced through both corneal surfaces to the best focus plane. Alternatively, a divergent bundle of rays starting, for example on-axis at a refractometry lane distance of 6 m could be used (Langenbucher et al. 2020). By accumulation of the optical path length from object to image (through air, cornea and aqueous humour), we were able to directly read out the optical path length differences for all the rays, which refer to the optical aberration (in μm). If we reference the best focal plane to the corneal front or back vertex plane, we can

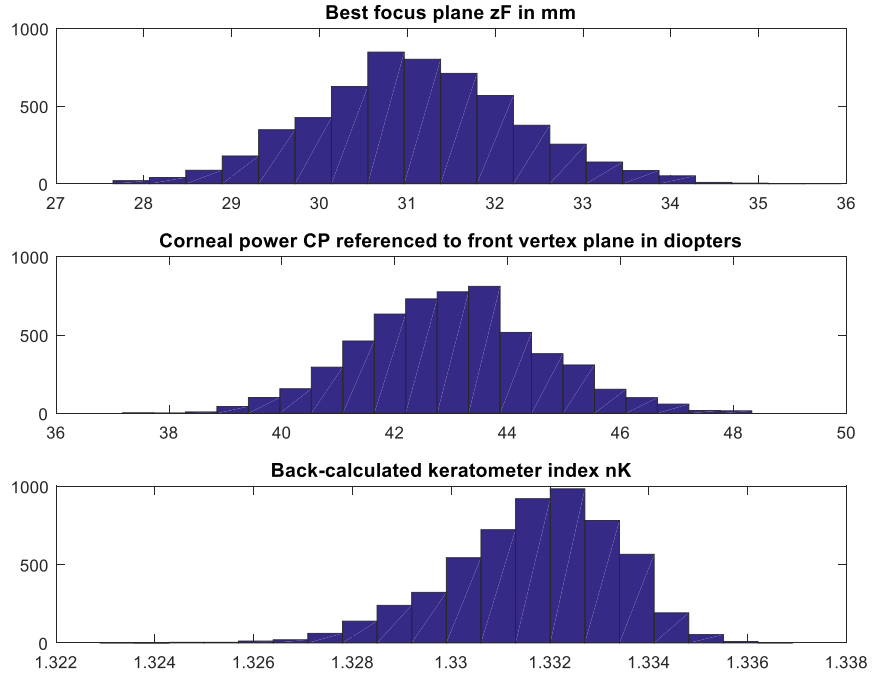

Fig. 2. Histogram of the distribution of output parameters ($N = 10{,}218$). $z = z_F$ refers to the best focus plane (plane with the lowest ray scatter), CP to the corneal power with respect to the corneal front vertex plane $z = 0$ derived from z_F and n_K to the back-calculated keratometer index.

easily derive the power of the cornea with respect to the front surface or back surface (Langenbucher et al. 2020). As we require corneal power with respect to the corneal front vertex plane for intraocular lens power calculation, we decided to use the term corneal power with the reciprocal of the distance from $z = 0$ to $z = z_F$ corrected for the refractive index of the aqueous humour.

In this paper based on a large dataset, we derived a focal length of around 31.2 mm behind the corneal front vertex, which refers to a corneal power of around 42.9 dioptres. On average, lateral ray scatter (root mean squared error) at the best focal plane was 3.32 µm, standard deviation of optical path length differences was 0.18 µm and the back-calculated keratometer index was 1.3317 on average. Considering that we used raytracing techniques and adapted the diameter of the ray bundle traced through the eye individually to the measured pupil size, the resulting keratometer index is very similar to that what was shown in the literature before (Fam & Lim 2007; Olsen & Jeppesen 2018; Langenbucher et al. 2020). In a recent study, we used paraxial calculation strategies based on a thick lens model and back-calculated the refractive index for clinical data after cataract surgery for a finite lane distance for refractometry and obtained a keratometer index of around 1.330 (Langenbucher et al. 2020). As the cornea shows some positive spherical aberration (in this study around 0.18 µm) which is not fully compensated by the typical prolate shape, it is obvious that the keratometer index here is somehow slightly higher compared to a paraxial assessment.

It was surprising to us that in the Monte Carlo simulation and the mono-variate assessment of the keratometer index as shown in Figure 3, only the front surface asphericity, seems to affect the keratometer index. For instance, the mono-variate model (as shown in model 3 for the corneal front surface radius) does not show any significant difference from a constant model. Even using corneal front and back surface radius and central corneal thickness, the regression model does not show a significant difference compared to the constant model (model 2). But if we use a multivariate regression analysis using all input parameters (R_a, Q_a, R_b, Q_b, CCT and PUP; model 1) the model shows a very good performance and therefore it seems that a proper estimate of the keratometer index is possible with this model.

In order not to overload this simulation, we restricted the analysis to a rotationally symmetric optical model (without decentration and tilt). Using that model, we characterized our dataset with 6 input parameters. In general, such a Monte Carlo simulation would be much more difficult if astigmatic surfaces or even free-form surfaces and misalignments such as decentration and tilt were included: firstly this would require 3D raytracing, and secondly we would require a general description of both surfaces instead of quadric surfaces which are more easily handled. Finally, it would no longer be possible to describe the results with a linear multivariate model (e.g. model 1 in this paper). Therefore, interpretation might be very complex.

Clinicians have to keep in mind that we could not ignore the variation of the keratometer index in general. Based on our dataset with $N = 10{,}218$ data points, we observed for n_K an individual variation of 1.3233 to 1.3390 and a standard deviation of 0.0017. This means, for example for an average corneal front surface curvature of 7.7 mm that considering the 2.5% and 97.5% quantile of the back-calculated keratometer index (1.3242 and 1.3371), in the worst-case scenario corneal power could be 324.2/7.7 = 42.17 dioptres or 337.1/7.7 = 43.78 dioptres (difference 1.67 dioptres). In reality, these extreme values are retrieved from extreme combinations of input parameters, and in normal cases the variation will be much smaller! A simple alternative to this raytracing-based calculation would be to use a straightforward paraxial model for thick lenses as shown in (Langenbucher et al. 2020), which considers at least the radius of curvature of both corneal surfaces and the central corneal thickness and could be applied with data from any modern optical biometer which measures the radii of both corneal surfaces (e.g. IOLMaster 700, Carl-Zeiss-Meditec, Jena, Germany).

In conclusion, we have shown with a raytracing-based calculation strategy applied to a large dataset of $N = 10{,}218$ measurements, how the back-calculated keratometer index varies with combinations of corneal front and back surface radius, corneal front and back surface asphericity, central corneal thickness and pupil size. Based

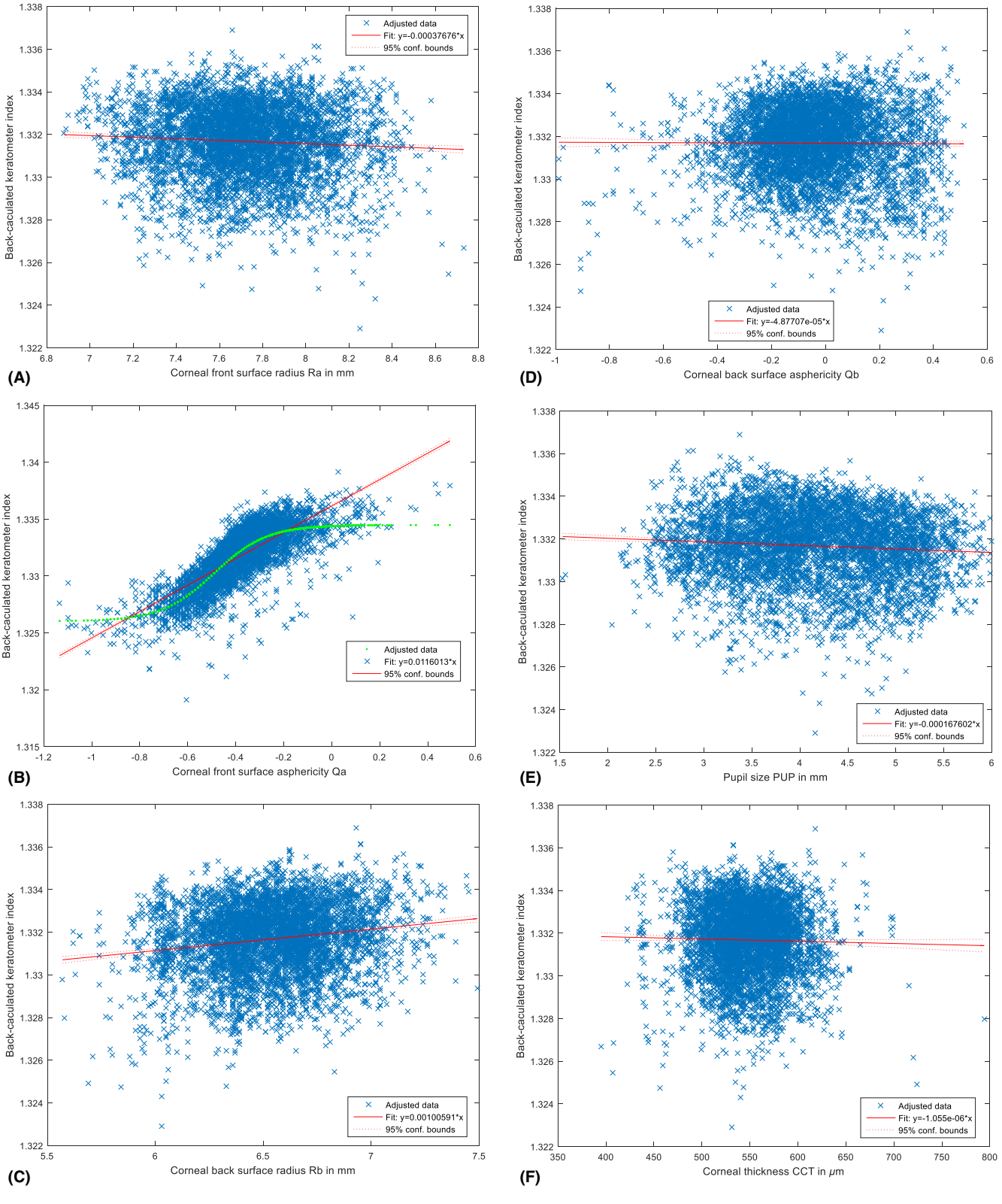

Fig. 3. Back-calculated keratometer index as a function of corneal front surface radius R_a (A), corneal front surface asphericity Q_a (B), corneal back surface radius R_b (C), corneal back surface asphericity Q_b (D), central corneal thickness CCT (E) and pupil size PUP (F). In addition to the data, the linear fit in terms of minimisation of the least squared fit error is displayed. In Figure 3B due to the distribution of the data a sigmoidal function was fitted. If we restrict to 1 effect size, only the asphericity of corneal front surface is usable for prediction of keratometer index.

on the best focus plane, we determined the corneal power and derived an individual keratometer index which translates the corneal front surface radius to the corneal power. We fitted a multiple linear regression model to this dataset, which shows a very good performance and which could be used to estimate the individual keratometer

index providing all input parameters are available.

References

Fam HB & Lim KL (2007): Validity of the keratometric index: large population-based study. J Cataract Refract Surg **33**: 686–691.

Haigis W (2012): Challenges and approaches in modern biometry and IOL calculation. Saudi J Ophthalmol **26**: 7–12.

Ho JD, Tsai CY, Tsai RJ, Kuo LL, Tsai IL & Liou SW (2008): Validity of the keratometric index: evaluation by the Pentacam rotating Scheimpflug camera. J Cataract Refract Surg **34**: 137–145.

Langenbucher A, Eberwein P, Fabian E, Szentmáry N & Weisensee J. (2020): Rückrechnung des Keratometerindex – Welcher Wert wäre bei der Kataraktchirurgie richtig gewesen? [Back-calculation of the keratometer index-Which value would have been correct in cataract surgery?]. Ophthalmologe. https://doi.org/10.1007/s00347-020-01182-7

Langenbucher A, Eppig T, Seitz B & Janunts E (2011): Customized aspheric IOL design by raytracing through the eye containing quadric surfaces. Curr Eye Res **36**: 637–646.

Langenbucher A, Haigis W & Seitz B (2004): Difficult lens power calculations. Curr Opin Ophthalmol **15**: 1–9.

Langenbucher A, Janunts E, Seitz B, Kannengießer M & Eppig T (2014): Theoretical image performance with customized aspheric and spherical IOLs – when do we get a benefit from customized aspheric design? Z Med Phys **24**: 94–103.

Langenbucher A, Szentmáry N, Spira C, Seitz B & Eppig T (2016): Hornhautbrechwert nach 'Descemet Stripping Automated Endothelial Keratoplasty' (DSAEK) - Modellierung und Konzept für die Berechnung von Intraokularlinsen [Corneal power after descemet stripping automated endothelial keratoplasty (DSAEK) – Modeling and concept for calculation of intraocular lenses]. Z Med Phys **26**: 120–126.

Langenbucher A, Viestenz A, Viestenz A, Brünner H & Seitz B (2006): Ray tracing through a schematic eye containing second-order (quadric) surfaces using 4 x 4 matrix notation. Ophthalmic Physiol Opt **26**: 180–188.

Levenberg K (1944): A method for the solution of certain problems in least squares. Quart Appl Math **2**: 164–168.

Liou HL & Brennan NA (1997): Anatomically accurate, finite model eye for optical modeling. J Opt Soc Am A Opt Image Sci Vis **14**: 1684–1695.

Marquardt D (1963): An algorithm for least-squares estimation of nonlinear parameters. SIAM J Appl Math **11**: 431–441.

Olsen T (1986): On the calculation of power from curvature of the cornea. Br J Ophthalmol **70**: 152–154.

Olsen T & Jeppesen P (2018): Ray-tracing analysis of the corneal power from Scheimpflug data. J Refract Surg **34**: 45–50.

Preussner PR, Wahl J & Weitzel D (2005): Topography-based intraocular lens power selection. J Cataract Refract Surg **31**: 525–533.

Received on September 29th, 2020.
Accepted on January 22nd, 2021.

Correspondence
Prof. Dr. Achim Langenbucher
Department of Experimental Ophthalmology
Saarland University
Kirrberger Str 100 Bldg. 22
66424 Homburg
Germany
Tel: +49 6841 1621218
Fax: +49 6841 1621240
Email: achim.langenbucher@uks.eu